A Novel Well Conditions Analysis Method through SFPI Algorithm

ZHENHUA SUN, XUEMIN TIAN
College of Information and Control Engineering
China University of Petroleum (East China)
No.271, Beier Road, Dongying
CHINA
tianxm@hdpu.edu.cn

Abstract: Through reviewing the popular time-frequency analysis methods of signals, this paper proposed a novel method with specific frequency polar images (SFPI) to process the electrical signals from beam-pumping unit motor due to the weakness of phase analyzing ability of the general time-frequency analysis methods. And the fundamental concept of the SFPI was defined. This method acquires the time-frequency distribution and phase information of signals by projecting them to a specific frequency polar. And through the dynamic tracks in the polar cycle, the time-frequency information was showed clearly. The SFPI was used to analyze the well conditions through motor electric signals. Finally, the characteristics of this method were concluded. And the direction of future works was assigned.

Keywords: Well conditions, Beam-puming unit, Dynamometer, Time-frequency, Specific frequency polar images

1 Introduction

The sinusoidal signal is the most popular signal in nature. It can be exactly formatted by three factors- amplitude, phase and frequency. In 1822, Fourier, an engineer of France, sponsored that a natural signal (denoted with $x(t)$) can be decomposed into a set of standard sinusoidal signals and the summation of them is just equal to the original signal. Fourier's theory became the foundation in the signal harmonic analysis field. A signal's information in frequency domain can be obtained through the Fourier Transform. This is very valuable to stationary signals analysis. But to non-stationary signals, it is difficult to obtain expected results by using the Fourier Transform analysis method only. As the frequency specification of a non-stationary signal is time varying and the Fourier Transform technique unable to locate the instantaneous frequency of a signal in its time domain, many valuable time-frequency analysis methods were studied. And the most common time-frequency analysis methods are Short-Time Fourier Transform, Wigner-Ville Distribution, Wavelet Transform, Hilbert-Huang Transform and Fractional Fourier Transform. In this article, a novel time-frequency analysis method based on the specific frequency polar images (SFPI) of a signal was introduced. Through this method a signal can be illustrated in a polar cycle and the dynamic tracks show more information of the signal's time-frequency information.

In petroleum industry, oil recovery is facing a technology innovation due to the rapidly increased requirements of the energy [1][2]. The need to increase oil production and reduce operating costs from wells requires an integrated analysis of the pumping system including the performance and interaction of all the elements: the surface equipment, the downhole equipment, the well bore and the reservoir. The analysis is to be based on data obtained at the surface without entering the well bore and must yield an accurate representation of conditions that exist at the surface, within the well bore, at the sand face and within the reservoir.[3][4]

There are several different methods to use the data obtained at the surface without entering the well bore [5][6]. Like three-phase flow meter, dynamometer, electrical signals of the motor [7]. Three-phase flow meters are expensive and the dynamometer is the most popular method to analyze the well conditions without disturbing the well bore [8].

To extremely increase the reliability of the sensors and the efficiency of the data, electrical signals of the motor become more and more attracted in the field. But the electrical signals are uneasy to be analyzed because of the indirect representation and possibility of numerous disturbing sources. How can we extract the valid information from the mixed signals? There are many time-frequency analysis methods and each has its own advantages and shortages.

2 Review of the time-frequency analysis method

In 1964, to analyze the instantaneous frequency information of a signal in its time domain, Gabor evolved the Fourier Transform into Short-Time Fourier Transform, which is also called Windowed Fourier Transform. It can be considered as a generalized filter. The mathematical expression of it is:

$$G(\omega,t)=\int_R x(\tau)g(\tau-t)e^{-j\omega\tau}d\tau \qquad (1)$$

$g(t)$ is the windowed function. It works as a limitation of the time window range. As we know, the time resolution and the frequency resolution can not be improved at the same time by this analysis method. They are contradictive.

Wigner and Ville proposed a time-frequency analysis method by using signals localized self-correlation function in 1940's. This method was called Wigner-Ville Distribution. It's expression is:

$$W_x(t,\omega)=\int_{-\infty}^{+\infty}x(u+\tau/2)x^*(u-\tau/2)e^{-j\omega\tau}d\tau \qquad (2)$$

In the year 1966，Cohen concluded a unified expression of signals time-frequency distribution [9]：

$$C_x(t,\omega:g)=$$
$$\frac{1}{2\pi}\iiint x(u+\tau/2)x^*(u-\tau/2)g(\theta,\tau)e^{-j(\theta t+\omega\tau-u\theta)}dud\tau d\theta$$
……(3)

In the equation above, t is the variant about of time, τ is the time delay, ω is the variant about of frequency, θ is the frequency delay, $g(\theta,\tau)$ denotes as the kernel function of distribution, $x(t)$ is a signal in complex field, $x(t+\tau/2)x^*(t-\tau/2)$ is the instantaneous self-correlation function of $x(t)$. The kernel function $g(\theta,\tau)$ plays a key role in this time-frequency analysis method and works as a band pass filter both in time domain and in frequency domain. When the $g(\theta,\tau)$ is equal to 1， the Cohen expression changed into Wigner-Ville Distribution. So the Wigner-Ville Distribution is the most simplified type of Cohen-Type distribution.

To the multi-fraction signals, the cross-term problem is unavoidable. Choi-Willams advised a type of experiential kernel function, $g(\theta,\tau)=e^{-\theta^2\tau^2/\sigma}$, and its time-frequency distribution is experiential. σ is a constant [10]. The greater the value of σ is, the higher the resolution of the self-correlation fraction. And the cross-term fraction is obviously restrained as the value of σ becomes smaller. Barkat advised a type of hyperbolical kernel function [11], $g(\tau)=\frac{1}{\cosh^2(\tau)}$. It has good behaviors in frequency spectrum converging.

In 1974, the concept of Wavelet Transform was submitted firstly by J.Morlet, a French engineer engaging in petroleum signals processing. After tens of years researching by scientists from the world, the mathematical system of Wavelet Transform was established. A strong theoretical principle was given to the applications of Wavelet Transform. Compared with Fourier Transform, Wavelet Transform is good at time-frequency analysis and multi-scale analysis. Through adjusting the value of relevant variants, the frequency resolution can be zoomed and the location of time can be moved separately. Both operations are smoothly. So some stubborn problems to Fourier Transform were easily solved by using Wavelet Transform analysis method.

The Wavelet Transform is a decomposing process of a signal based on a set of normal orthogonal basis [12]. And the mathematical expression of the transform is:

$$\{W_{2^j}x(t)\}=x(t)*\psi_{2^j}(t)=2^{-j}\int_R x(\tau)\psi\left(\frac{t-\tau}{2^j}\right)d\tau$$
……(4)

In the equation above, $\psi_{a,b}(t)=|a|^{-\frac{1}{2}}\psi\left(\frac{t-b}{a}\right)$ is a set of orthogonal wavelet basis function. The Wavelet Transform has many good specifications such as the focusing ability, easy to restructure. But the frequency leakage caused by data shortening still affects the analysis results.

A natural signal $x(t)$ can construct its own analytic terms by Hilbert Transform.

$$z(t) = x(t) + j\hat{x}(t) = a(t)e^{j\varphi(t)} \quad (5)$$

Here, $\hat{x}(t)$ denotes the Hilbert Transform of $x(t)$, and its definition is:

$$\hat{x}(t) = \frac{1}{\pi}\int_{-\infty}^{\infty} \frac{x(\tau)}{t-\tau} d\tau = x(t) * \frac{1}{\pi t} \quad (6)$$

Suppose the frequency fractions of $a(t)$ and the complex sinusoid $e^{j\varphi(t)}$ were fully separated at any time location, in another words they were independence with each other in frequency domain, $a(t)$ was considered as the envelope of $z(t)$. $\varphi(t)$ is the phase angle, $f(t) = \frac{1}{2\pi}\frac{d\varphi(t)}{dt}$ is the instantaneous frequency of signal $x(t)$.

Thus the amplitude and the phase information of the signal were fully expressed. In general, a natural non-stationary signal was difficult to satisfy the above supposition. So the $a(t)$ and $e^{j\varphi(t)}$ obtained by Hilbert Transform can easily induce serious frequency spectrum aliasing. To solve this problem, Huang proposed the Hilbert-Huang Transform in 1998 [13]. There are two important definitions of Hilbert-Huang Transform. One is EMD（Empirical Mode Decomposition）, the other is IMF(Intrinsic Mode Functions). The definition of IMF is the fundamental conditions to use the Hilbert Transform. It was satisfied with the supposition and the EMD is a valid tool to get IMFs. The Hilbert-Huang Transform has good application although its mathematic explaining is insufficiency. And there is another shortage of Hilbert-Huang Transform. When some small local fluctuations appeared, the EMD was difficult to find them. It can bring the wave mixing phenomenon on [14]. Thinking about that this shortage was only arose from some small local independent waves, Dr. Wu attempted to add noises in the data in order to separate those small fluctuations out firstly, and then filter the noises from the result. This method is called EEMD (Ensemble EMD) [15]. To get the envelope, it must calculate the cubic spline interpolation repeatedly and will consume a great mount of time.

In summarize, some algorithms are of simplicity but less resolution of the results, some algorithms are better resolution but cost a lot of time to compute. In order to get more information about the phase in signal analysis, a method based on images of the signals was introduced.

3 Concept of the SFPI

To a continuous signal $x(t)$, its Fourier Transform can expressed by:

$$X(j\omega) = \int_{-\infty}^{+\infty} x(t)e^{-j\omega t} dt \quad (7)$$

Convert it into vector expression:

$$X(j\omega) = A(\omega)e^{j\theta(\omega)} \quad (8)$$

Then the phase angle of $x(t)$ is $\theta(\omega)$ at frequency ω. Supposed $x(t)$ is a stationary signal, its time-frequency distribution can expressed by:

$$C(t,\omega) = e^{j\omega t} X(j\omega) = A(\omega)e^{j(\omega t + \theta(\omega))} \quad (9)$$

Because of the Fourier Transform translate the frequency information of signals in whole time area, formation (9) is only available to periodic stationary signals. To a non stationary signal, the result is implicit.

Take the equation (7) into equation (9), we can get:

$$C(t,\omega) = e^{j\omega t}\int_{-\infty}^{+\infty} x(\tau)e^{-j\omega\tau} d\tau \quad (10)$$

Suppose the local cycle time of the signal is T, then $\omega = \frac{2\pi}{T}$, the equation above was transformed into:

$$C(t,T) = \int_{-\infty}^{+\infty} x(\tau)e^{j\frac{2\pi}{T}(\tau - t)} d\tau \quad (11)$$

To reflect the local characteristics of the signal, one cycle integral area was established in order to give a standard polar image. Then we got:

$$C(t,T) = \int_{0}^{T} x(t-\tau)e^{j\frac{2\pi\tau}{T}} d\tau \quad (12)$$

The equation above has natural physical meanings. To show it explicitly, we use the concept of specific frequency polar images to illustrate it.

If a sinusoidal signal's cycle time is T, we establish a polar coordinate with the frequency of a cycle is $1/T$. Taking the amplitude calculated by equation (12) as radius and the phase as angle to make drawing, the track is just the specific frequency polar.

Thus we define $C(t,T) = \int_T x(t-\tau)e^{j2\pi\tau/T} d\tau$ as the specific frequency polar imaging of $x(t)$. Suppose $x(t) = \sin(t)$, then the tracks of the imaging at $T = 2\pi$ specific frequency polar is a unit circle. The image at different frequency polar of a real signal reflects its instantaneous frequency and phase information.

Transform equation (12) to vector expression:

$$C(t,T) = A(t,T)e^{j\theta(t,T)} \tag{13}$$

$A(t,T)$ is the amplitude and $\theta(t,T)$ is the phase angle of the SFPI result. Taking the $A(t,T)$ as radius and $\theta(t,T)$ as the angle, draw points on the polar, and make a line goes with the time t. Here the image we got just is the SFPI of the signals at $T = 2\pi$.

To meet the convenience of the computer calculating, we must use the discrete algorithm of the SFPI.

A time sequence signal: $X(i), i = 1,2,3,\cdots,n$. N is the specified steps of the signals.

$$C(n,N) = \frac{1}{N}\sum_{i=1}^{N} X\left[(n-i)e^{j2\pi i/N}\right] \tag{14}$$

and its vector expression is:

$$C(n,N) = A(n,N)e^{j\theta(n,N)} \tag{15}$$

As taking the specific frequency polar as reference, the different frequency fractions of $x(t)$ were imaged on the polar abided by the specific rules. From the images, it is extreme possible to estimate the time-frequency distribution and to locate the exact phase point at specified frequency. This method determined the scale of the time, appointed the location of the start point of the phase, and gave out the basis references to the measurement of frequency and phase. It has the advantages of intuitive, easy to image, four quadrant analysis and response in full frequency domain. Also to the reason of multi-scale frequency polar images, the difficulties arose by frequency leakage and the edge effecting problems were alleviated.

4 Analysis and simulation

Several different signals were constructed in order to view their characteristics of the specific frequency polar images.

At the system of polar coordinates, the signals processed by SFPI are imaged through taking the $A(t,T)$ as radius and $\theta(t,T)$ as the angle.

Fig.1 shows the track of the images of sin(t) at $T = 2\pi$ specific frequency polar. The amplitude becomes a constant. Laying the curve into a X-Y coordinate, it shows as a straight horizon line, the modulate information was filtered fully.

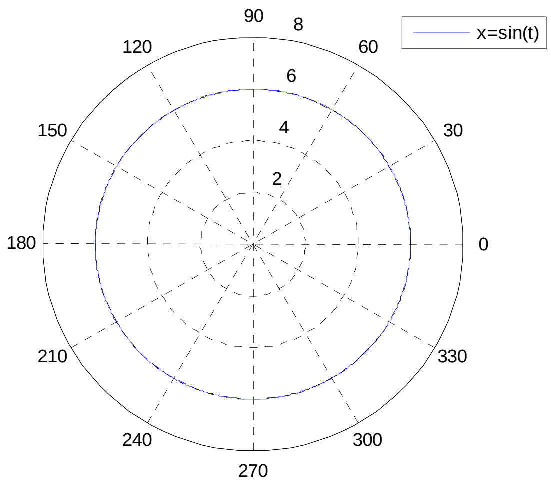

Fig. 1 The SFPI track of the sin(t)

Along with the increase of the frequency of the signals, the images resulted from SFPI were changed. Fig.2 shows the tracks of sin(2t) at $T = 2\pi$ specific frequency polar. The amplitude decreased rapidly. It cycled two times and showed as ellipses. These ellipses coincide.

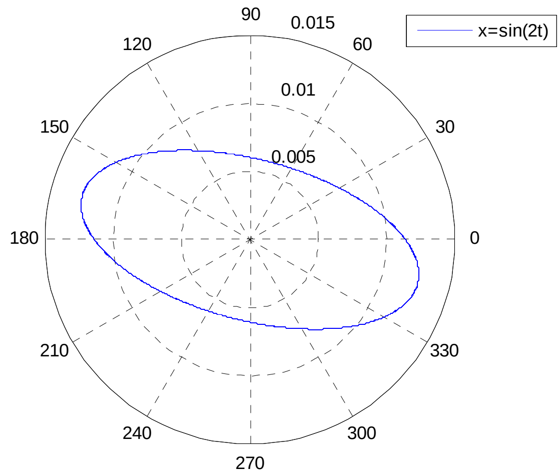

Fig. 2 The SFPI track of the sin(2t)

Making the further increase of the frequency of the signals, the ellipses become thinner and thinner. Fig.3 shows the tracks of sin(4t) at $T = 2\pi$ specific frequency polar. It cycled four times and showed as thin ellipses. Also these ellipses fully coincide.

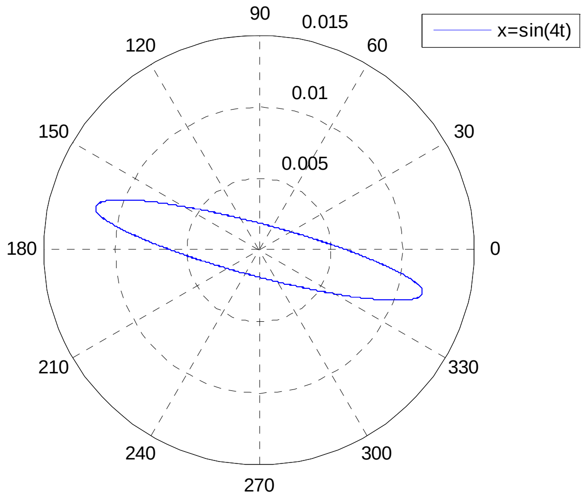

Fig. 3 The SFPI track of the sin(4t)

Decreasing the frequency based on the specific frequency of the SFPI, for example half of the base, the curve tracks a incomplete ellipse. Fig.4 shows the tracks of sin(t/2) at $T=2\pi$ specific frequency polar.

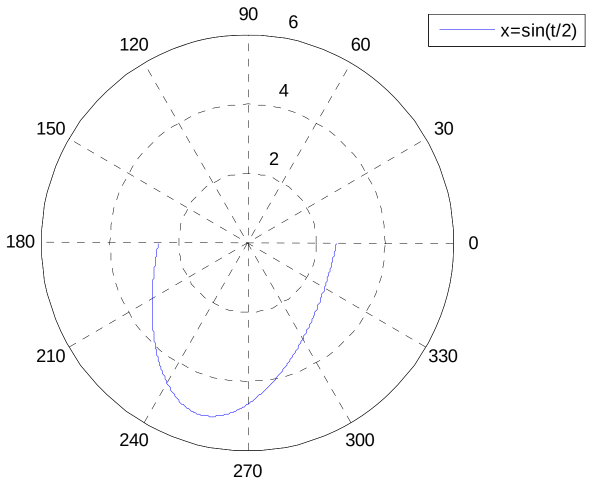

Fig. 4 The SFPI track of the sin(t/2)

If the signals were comprised of several different frequency fractures, the behavior of the images becomes complex, especially with vicinal performance between them. Fig.5 shows the tracks of sin(t/2)+ sin(t)at $T=2\pi$ specific frequency polar.

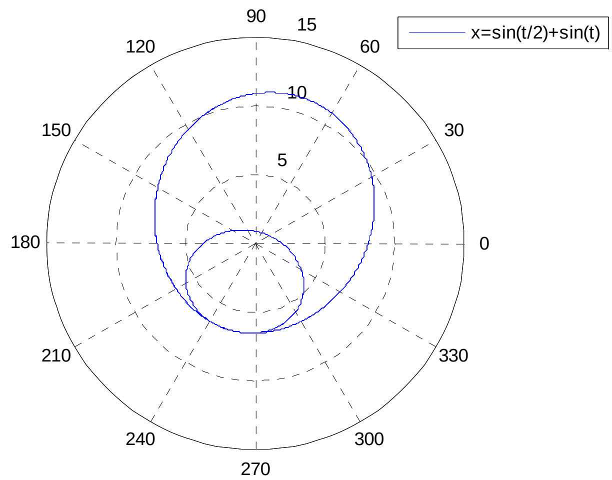

Fig. 5 The SFPI track of the sin(t/2)+ sin(t)

When the fractures were independent each other, they could be identified by the behavior of themselves. Fig.6 shows the tracks of sin(11.5t)+ sin(t)at $T=2\pi$ specific frequency polar.

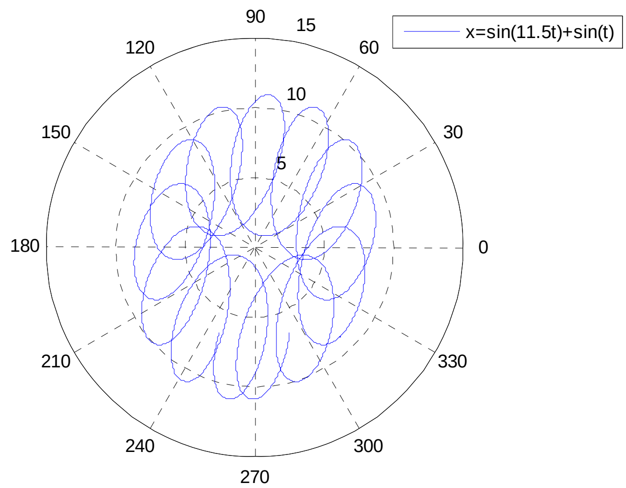

Fig. 6 The SFPI track of the sin(11.5t)+ sin(t)

Specification analyzing:

- To sinusoidal signals with unique base frequency, their images are standard circles, and the circle founded time is the defined basic cycle time.
- To sinusoidal signals with non-unique base frequency, their images are ellipses, and the ellipse founded time is vary along with the different defined basic cycle time.
- The images disappeared when the frequency of

the signal was integral multiples of base frequency. And the amplitude and phase affected each other but have a state correlation ship.

- The frequency lower than the base was restrained and the direct-current signal will be restrained completely. As $x(t)$ =constant, $C(t,T)=\int_T x(t-\tau)e^{j2\pi\tau/T}d\tau$=0.
- The images of the same signal behaved diversely at different specific frequency polar. But the trends of the images have strong regulations. Recognizing the regulations will be the most important works of the future.
- The SFPI algorithm acts as a weighted mean filter in mathematics.

5 Application in well conditions analysis

Downhole pump conditions exert as much influence on system behavior and surface loading as do the beam unit, prime mover and rod string [16]. Electrical parameters and power costs appear to reflect the behaviors indirectly. Fig. 7 shows the scheme of the artificial lifting oil recovery with the Beam-Pump Unit. Traditional method to get the downhole information mainly uses the dynamometer at the loading point [17][18]. It reflects the changes of the loading directly and plays an important role in the past decades years. But because of the install position of the loading sensor is mobile, the instrument was damaged frequently and this due to a heavy burden of maintenance. Also with the heavy load of sensor supported, the measuring result of the sensor is easy drifted. Due to the lack of the efficient analysis methods, the electrical parameters and power costs were only used to verify the balance of the counter in the past [19]. Naturally, they can reflect the downhole conditions either. And there are problems to implement this task. One is how to get the exact torque and speed of the prime mover [20][21]. The other is what data analysis methods can extract the valid information from the vast mixed signals [22][23].

We can notice that the counter of the Beam-Pumping unit is fixed and regular. Also the other mechanical parts at the surface show the same characteristics. For this reason, a specified filter parameter can work efficiently.

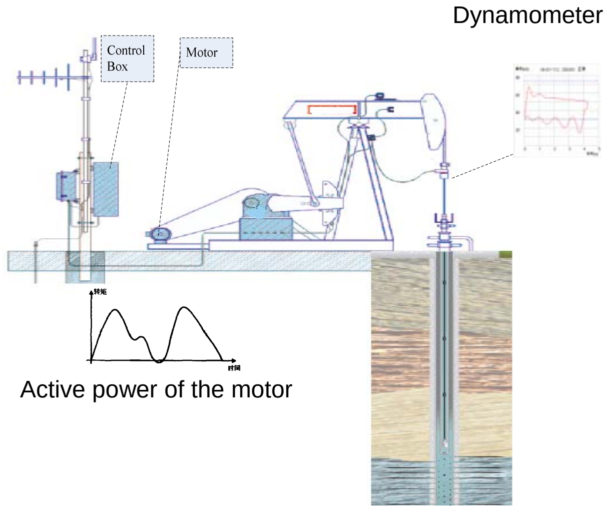

Fig. 7 Scheme of artificial lifting oil recovery with the beam-pump Unit

Firstly we can use the SFPI method to process the electrical signals of the motor.

To calculate the precise instantaneous value of the active power or the electromagnetic torque of a three phase asynchronous motor, the phase difference between the voltage and the current is the necessary parameter [24]. Fig. 8 shows the curves of the voltage, current and speed pulse sampled from an on-use motor which drives the Beam-Pumping unit. The horizontal ordinate represents the sample sequences and the vertical ordinate represents the value acquired with A/D converter. The data was sampled by a high-speed sample module at 200KHz. To balance the effect between the performance and cost of the system, a low cost data acquisition system was selected. Here can only get the deficient period signals and the sample process is intermittent. This type of signals brings the difficulty to analyze. Several methods were attempted [25]. The results were not ideal.

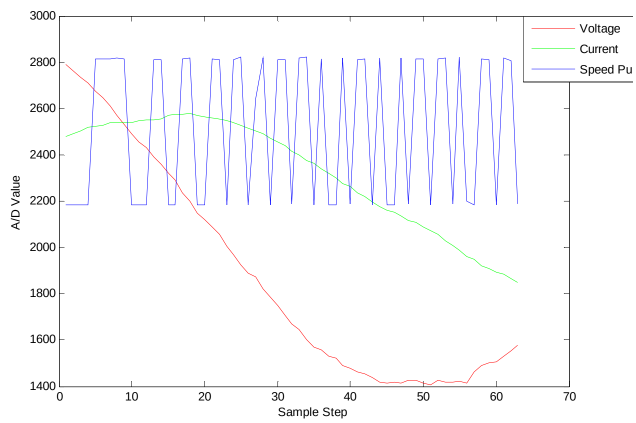

Fig. 8 The voltage, current and rotor speed signals of an on-run 3-Phase Asynchronous Motor

Here we use the SFPI algorithm to analyze the phase information of this type of signals. Through equation (14) and (15), calculate the amplitude and phase angle of the voltage and the current separately. Fig. 9 shows the amplitude of the voltage and current calculated by SFPI.

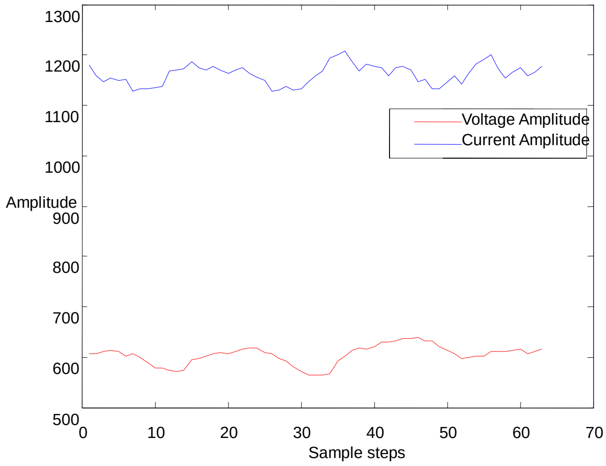

Fig. 9 The amplitude of the voltage and current calculated by SFPI

Fig. 10 shows the phase angle of the voltage and current calculated by SFPI.

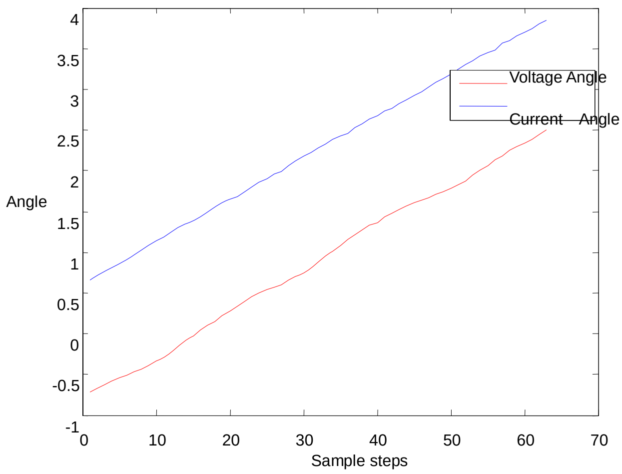

Fig. 10 The phase angle of the voltage and current calculated by SFPI

The phase difference between the voltage and the current is not the value of direct subtraction of them because of the voltage sampled is line voltage and the sampled current is phase current. Natural there true phase difference must subtract $\pi/6$ radius again based on their original obtained value.

So the ultimate value of the phase difference between the voltage and the current was illustrated in Fig. 11. It can be used to calculate the instantaneous power or torque, even estimate the rotor speed through motor models.

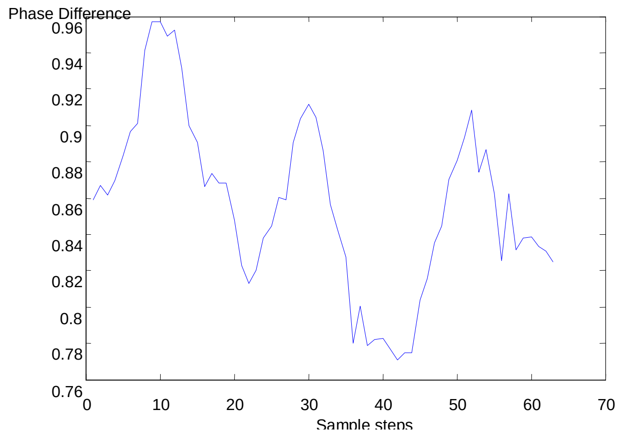

Fig. 11 The phase difference between the voltage and current calculated by SFPI

Also, they can be showed as an image to the specific polar, the trace is dynamic. And the comparison at different periods of the signals is clearly perceptible. So we can observe the changes easily. Fig. 12 shows the image.

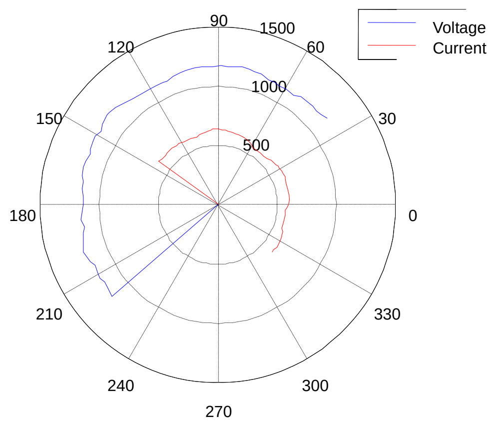

Fig. 12 The voltage and current images to the specific polar

Since we get the power or the torque of the motor, we can analyze them to acquire the well conditions at downhole position. But it is very difficult to acquire useful information through the data directly like Fig. 13. This is a real-time active power data sampled from a motor which drives a running beam-pump unit.

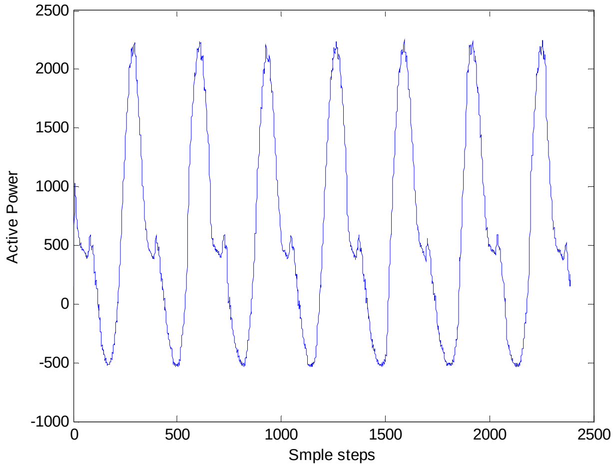

Fig. 13 A real-time active power curve of a beam-pump unit driven motor

At the beam-pump unit running time, there are maybe a lot of things to be happened, like fluid pounding, gas interference, pump or tubing leakage, parted rods, friction, etc. At most time, they leave imprints on the dynamometer or the electrical curve showed at Fig. 7. The field engineer inspects the images and makes decisions what things have happened downhole. The dynamometer has the superiority to the electrical curves at showing downhole conditions. But the instrument served for it is more vulnerable. And with the trivial floating of the conditions, it is uneasy to percept through the dynamometer because of the original heavy load to the sensor. To electrical signals, the balance plays the positive roll to increase the resolution of the results.

As the Fig. 13 showed, the changes of the conditions were uneasy to percept at the rapidly evolving styles. Translating it into Fig. 14 through SFPI algorithm, the changes were amplified.

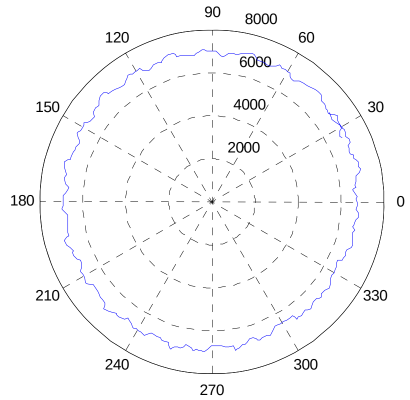

Fig. 14 The SFPI in one specific period of the power signal.

Plot the amplitude into X-Y coordinate. See in Fig. 15.

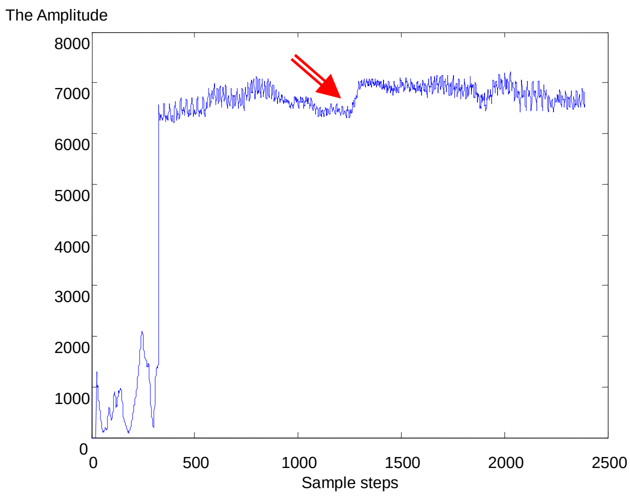

Fig. 15 The amplitude of the SFPI results

In Fig. 15, the red arrow shows the work conditions changed clearly. From Fig. 13 we can also find the trace of the changes, but it is impossible to do that if you are not careful.

Fig. 16 shows the phase angle of the SFPI results.

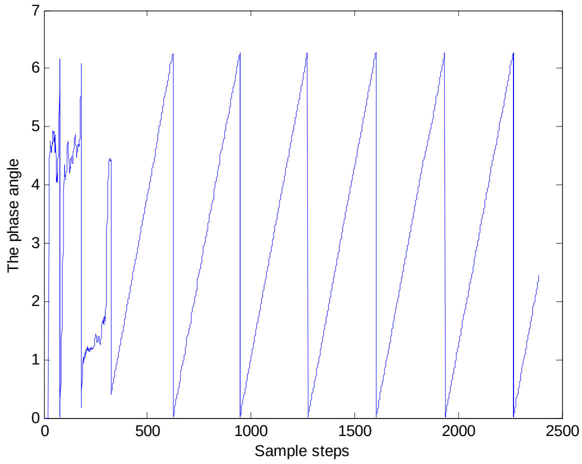

Fig. 16 The phase angle of the SFPI results

The phase angle gives the time or space reference to the results and it has extra useful function to the signal analysis.

6 Conclusion

The time-frequency distributions of signals are intricate in reality. Images can express more information than the numbers. So the author constructed the specific frequency polar to project the signals on it by the specified method. This analysis method is based on intrinsic frequency characters. It can inspect the images specifications at different frequency polar. And connect them with the time-frequency distribution and phase information. It is intuitive, easy to understand and recognize the regulation of their specifications and then provides a novel ways to time-frequency analysis. Through the application to the downhole conditions of a beam-pumping unit, it is testified that the SFPI method works well. But this method is on the research stage now. It has a lot of things to do at the future. Next the performance evaluation will be studied. The quantization and mathematical expression must be deduced.

References:

[1] M. A. R. CANELON, E. C. MORLES. Fuzzy Clustering Based Models Applied To Petroleum Processes. *WSEAS TRANSACTIONS on SYSTEMS and CONTROL,* Vol. 3 No. 3 Mar. 2008, 159-171.

[2] M. A. R. Canelón, J. Dávila, E. C. Morles. INTELLIGENT SUPERVISION OF PETROLEUM PROCESSES BASED ON MULTI-AGENT SYSTEMS. *WSEAS TRANSACTIONS on SYSTEMS and CONTROL,* Vol. 4 No. 9 Sep. 2009, 435-444.

[3] A.L. Podio, J. N. McCoy, Dieter Becker, Lynn Rowlan and Bill Drake.Total Well Management II. *SPE67273*, 2001.

[4] J. N. McCoy, A.L. Podio, Bill Drake, Lynn Rowlan.Modern Total Well Management - Sucker Rod Lift Case Study. *SPE68864*, 2001.

[5] S.G. Gibbs. A General Method for Predicting Rod Pumping System Performance. *SPE 6850*,1977.

[6] Alegre.L, Petrobras S.A., C. K. Morooka and A, F. Rocha. Intelligent Diagnosis of Rod Pumping Problems. *SPE26516*, 1993.

[7] S.G. Gibbs. Utility of Motor-Speed Measurements in Pumping-Well Analysis and Control . *SPE13198*, 1987.

[8] D. Rogers, C.G. Guffey, and W.J.B. Oldiiam. Artificial Neural Net works for Identification of Beam Pump Dynamometer Load Cards. *SPE20651*, 1990.

[9] Cohen L. *Generalized phase-space distribution function*. J. of Math. Phys. , 1966,(7):781-786.

[10] Choi H L,Willams W J. Improved time-frequency representation of multi-component signals using exponential kernels. *IEEE Trans. on ASSP*, 1989,37(6):862-871.

[11] Barkat B, Boashash B. A High-resolution quadratic time-frequency distribution for multi-component signals analysis[J]. *IEEE Transaction on Signal Processing*, 2001, 49(10): 2232-2239.

[12] N. VINCENZO, Q. GIUSEPPE, F. ANIELLO. The detection of gear noise computed by integrating the Fourier and Wavelet methods. *WSEAS TRANSACTIONS on SIGNAL PROCESSING*, Vol. 4 No. 3 Mar. 2008, 60-67.

[13] N.E. Huang, Z. Shen, S.R. Long, M.C. Wu, H.H. Shih, Q. Zheng, N.C. Yen, C.C. Tung, and H.H. Liu, *The empirical mode decomposition and the Hilbert spectrum for nonlinear and non-stationary time series analysis*, Proc. Royal Soc. Lond. A454(1998), 903-995.

[14] V. Vatchev, *Intrinsic Mode Functions and the Hilbert Transform*, Ph.D Dissertation, Department of Mathematics, University of South Carolina, 2004.

[15] Z.H. Wu and N.E. Huang, A study of the characteristics of white noise using the empirical mode decomposition method, *Proceedings of the Royal Society of London* 460A (2004), pp. 1597–1611.

[16] O.Lynn Rowlan,James F.Lea,etc. Overview of Beam Pump Operations. *SPE110234*, 2007.

[17] Roderick R. Dickinson, James W. Jennings. Use of Pattern-Recognition Techniques in Analyzing Downhole Dynamometer Cards. *SPE Production Engineering*, May 1990.

[18] Kenneth B. Nolen, and Sam G. Gibbs . Quantitative

Determination of Rod-Pump Leakage with Dynamometer Techniques. *SPE Production Engineering*, August 1990.

[19] J.N. McCoy, R.E. Ott, A.L. Podio, Forrest Collier and Dieter Becker. Beam Pump Balancing Based on Motor Power Utilization. *SPE29533*, 1995.

[20] J. Li, L. Xu, Z. Zhang, An adaptive sliding-mode observer for induction motor sensorless speed control *IEEE Transactions on Industry Applications,* Vol. 41 No. 4 July-Aug. 2005, 1039-1046.

[21] I. I. SILLER-ALCALÁ, M. ABDERRAHIM, J. JAIMES-PONCE, AND R. ALCÁNTARA-RAMÍREZ. Speed-Sensorless Nonlinear Predictive Control of a Squirrel Cage Motor. *WSEAS TRANSACTIONS on SYSTEMS and CONTROL*, Vol. 3, ,No. 2 Feb 2008, 99-104

[22] J. J. Medel Juárez, J. C. García Infante, J. C. Sánchez García. Real-time Neuro-fuzzy Digital Filtering: Basic Concepts. *WSEAS TRANSACTIONS on SYSTEMS and CONTROL,* Vol. 3 No. 8 Aug. 2008, 663-654.

[23] DURSUN ÜSTÜNDAĞ, MEHMET CEVRİ. Estimating Parameters of Sinusoids from Noisy Data Using Bayesian Inference with Simulated Annealing. *WSEAS TRANSACTIONS on SIGNAL PROCESSING,* Vol. 4 No. 8 Aug. 2008, 432-441.

[24] YAO Hai-yan, CHEN You-long, LIU Jian-feng. Study of High-Precision Method for Measuring the Small Difference of Phase, *Metrology & Measurement Technique*, 2008,35(8)：29-31.

[25] Sun Zhen-Hua, Tian Xue-Min, Wang Ping. A novel signals splitting method for intermittent sampling in deficient period[C]. *Proceedings of 2008 3rd International Conference on Intelligent System and Knowledge Engineering,* ISKE 2008, p 656-661, 2008.